Structure−Activity Analysis of a *Conus* Peptide Blocker of N-Type Neuronal Calcium Channels

Laszlo Nadasdi,* Donald Yamashiro, David Chung, Katalin Tarczy-Hornoch, Peter Adriaenssens, and J. Ramachandran

Neurex Corporation, Menlo Park, California 94025

Received April 6, 1995; Revised Manuscript Received April 26, 1995[⊗]

ABSTRACT: The synthetic peptide SNX-111 corresponding to the sequence of the ω-conopeptide MVIIA from the venom of the marine snail *Conus magus* is a highly potent and selective antagonist of N-type calcium channels. We have synthesized and characterized a large number of analogs of SNX-111 in order to elucidate the structural features of the peptide involved in blocking N-type calcium channels. Comparison of the binding of SNX-111 and its analogs to rat brain synaptosomal membranes rich in N-type channels revealed that, among the four lysines and two arginines in the molecule, lysine in position 2 and arginines at position 10 and 21 are important for the interaction of SNX-111 with N-type channels. The importance of the middle segment from residues 9 through 14 for this binding interaction was revealed by substitution of the individual residues as well as by the construction of hybrid peptides in which the residues 9−12 in SNX-111 and another conopeptide, SNX-183, corresponding to a peptide SVIB from *Conus striatus*, were interchanged. Introduction of the sequence SRLM from SNX-111 in place of RKTS in position 9−12 in SNX-183 resulted in a 38-fold increase in affinity.

Recent molecular cloning strategies have revealed a much larger diversity of neuronal voltage sensitive calcium channels (VSCC)[1] than previously recognized on the basis of electrophysiological properties (Tsien et al., 1991; Snutch and Reiner, 1992; Miller, 1992). The ω-conopeptides found in the venoms of fish-eating marine snails are becoming highly useful tools in the characterization of the novel neuronal VSCC (Olivera et al., 1990, 1994; Hillyard et al., 1992; Ramilo et al., 1992; Ramachandran et al., 1993; Olivera et al., 1994). The synthetic peptide SNX-111, corresponding to the structure of the ω-conopeptide MVIIA from *Conus magus*, a highly selective and potent blocker of N-type VSCC (Olivera et al., 1987; Ramachandran et al., 1993), has also been found to be an effective neuroprotective agent in animal models of transient global ischemia (Smith & Siesjo, 1992; Valentino et al., 1993) as well as focal ischemia (Xue et al., 1993; Buchan et al., 1994). Selective blockage of N-type VSCC with SNX-111 has also been shown to be potently antinociceptive in animal models of pain syndromes (Gohil et al., 1993). We have synthesized and characterized a number of analogs of SNX-111 in order to elucidate structural features of the molecule responsible for the high binding affinity to purified synaptosomes. Although it has been pointed out, that the relationship between the binding affinity, the channel specificity, and the blocking efficacy could be complex for different toxins (Oliveria et al., 1994), throughout this paper we assumed that for closely related analogs of a particular peptide like SNX-111 the N-type VSCC blocking potency and the brain synaptosomes binding potency are strongly related.

The ω-conopeptides are highly basic peptides ranging in size from 24 to 29 amino acid residues, folded into compact, rigid structures through three intramolecular disulfide bridges (Gray et al., 1988; Olivera et al., 1994). The sequences between the invariant cysteine residues are highly variable; only glycine at position 5 is conserved (Ramilo et al., 1992). SNX-111 has 25 amino acid residues and a net charge of +6. The importance of each of the four lysines and two arginines in the sequence of SNX-111 was analyzed by replacing each basic residue with an alanine residue. Partial enzymatic cleavage of SNX-111 with chymotrypsin as well as amino acid residue substitution were employed to assess the role of the middle segment between cysteine 8 and cysteine 15. The importance of residues 9−12 in the middle segment was evaluated by constructing hybrid molecules in which the residues 9−12 in SNX-111 were replaced by the corresponding residues from another ω-conopeptide, SVIB (SNX-183), derived from *Conus striatus* (Ramilo et al., 1992). The amino acid sequences of all the synthetic peptides used in this investigation are shown in Table 1.

EXPERIMENTAL PROCEDURES

Materials. MBHA resin (styrene cross-linked with 1% divinylbenzene, 100−200 mesh size, substitution level 0.5−0.7 mequiv/g) and Boc-amino acid derivatives were purchased from Bachem California (Torrance, CA) or Advanced ChemTech (Louisville, KY). DCC was obtained from Fluka (Ronkonkoma, NY); HOBt, DIEA, and DTT from Aldrich (Milwaukee, WI); HF from Linde (San Jose, CA); and TFA from Halocarbon (River Edge, NJ). HOBt was recrystallized from chloroform/tetrahydrofuran. DIEA was dried over KOH and distilled. TFA was distilled from glycine (2 g/L), and dioxane was distilled from $NaBH_4$ (4 g/L). IPM was prepared as described (Yamashiro & Li, 1988).

Instruments. The peptides were synthesized on a Model 430A automatic synthesizer (ABI, Foster City, CA), and

* To whom correspondence should be addressed.

[⊗] Abstract published in *Advance ACS Abstracts,* June 1, 1995.

[1] Abbreviations: MBHA, 4-methylbenzhydrylamine resin; DCC, *N,N'*-dicyclohexyl carbodiimide; HOBt, 1-hydroxybenzotriazole; DCM, methylene chloride; DMF, *N,N'*-dimethylformamide; DIEA, diisopropylethylamine; TFA, trifluoroacetic acid; IPM, *N*-isopropylmorpholine; ACN, acetonitrile; IPA, isopropyl alcohol; DTT, dithiothreitol; Nle, norleucine; ITyr, 3-iodotyrosine; VSCC, voltage-sensitive calcium channel; HPLC, high-pressure liquid chromatography. The abbreviations for amino acids are according to IUPAC−IUB recommendation.

0006-2960/95/0434-8076$09.00/0

Table 1: Amino Acid Sequences of SNX-111 and Synthetic Analogs

SNX-111		C	K	G	K	G	A	K	C	S	R	L	M	Y	D	C	C	T	G	S	C		R	S	G	K	C
SNX-183		-	-	L	-	-	Q	S	-	R	K	T	S	-	-	-	-	S	-	-	-	G	-	-	-	-	-
SNX-190		-	-	-	A	-	-	-	-	-	-	-	-	-	-	-	-	-	-	-	-		-	-	-	-	-
SNX-191		-	A	-	-	-	-	-	-	-	-	-	-	-	-	-	-	-	-	-	-		-	-	-	-	-
SNX-194		-	-	-	-	-	-	-	-	-	-	-	*a*	-	-	-	-	-	-	-	-		-	-	-	-	-
SNX-195		-	-	-	-	-	-	-	-	-	-	-	-	-	-	-	-	-	-	-	-		-	-	-	A	-
SNX-198		-	-	-	-	-	-	-	-	-	-	-	-	-	-	-	-	-	-	-	-		A	-	-	-	-
SNX-199		-	-	-	-	-	-	-	-	-	A	-	-	-	-	-	-	-	-	-	-		-	-	-	-	-
SNX-200		-	-	-	-	-	-	A	-	-	-	-	-	-	-	-	-	-	-	-	-		-	-	-	-	-
SNX-201		-	-	-	-	-	-	-	-	R	K	T	S	-	-	-	-	-	-	-	-		-	-	-	-	-
SNX-202		-	-	L	-	-	Q	S	-	-	-	-	-	-	-	-	-	S	-	-	-	G	-	-	-	-	-
SNX-220	Ac-	-	-	-	-	-	-	-	-	-	-	-	-	-	-	-	-	-	-	-	-		-	-	-	-	-
SNX-257		-	-	-	-	-	-	-	-	-	-	-	-	F	-	-	-	-	-	-	-		-	-	-	-	-
SNX-259		-	-	-	-	-	-	-	-	-	-	-	-	*b*	-	-	-	-	-	-	-		-	-	-	-	-
SNX-273		-	-	-	-	-	-	-	-	-	-	-	A	-	-	-	-	-	-	-	-		-	-	-	-	-
SNX-279		-	-	-	-	-	-	-	-	-	-	-	*c*	-	-	-	-	-	-	-	-		-	-	-	-	-
SNX-288		-	-	-	-	-	-	-	-	-	-	A	-	-	-	-	-	-	-	-	-		-	-	-	-	-
SNX-308		-	-	-	-	-	-	-	-	-	-	-	-	A	-	-	-	-	-	-	-		-	-	-	-	-

[a] Nle. [b] ITyr. [c] Met(O).

cleaved from the resin in an HF cleavage apparatus (Immuno Dynamics, San Diego, CA). Analytical-scale HPLC analyses were performed on Model 2350/2360 (ISCO, Lincoln, NE) and Model 1090 (Hewlett-Packard, Palo Alto, CA) systems. Preparative HPLC purification of the peptides was performed on a Rabbit (Rainin, Emeryville, CA) five-pump system (each pump equipped with a 50 mL/min maximal flow-rate pump head). Amino acid analysis was carried out on Model 119C amino acid analyzer (Beckman, Palo Alto, CA) using postcolumn ninhydrin derivatization.

Synthesis, Purification, and Characterization of Peptides. The peptides were synthesized according to programs developed in our laboratory using HOBt/DCC activation and a double coupling protocol for Arg, Asn, and Gln and symmetrical anhydride activation with single or double coupling protocol for all the other amino acids. The coupling protocol followed Yamashiro and Li (1988) with the exception that the symmetrical Boc-amino acid anhydrides were prepared on the synthesizer prior to the couplings.

The peptides were cleaved from the resin by liquid HF (1 mL of *p*-cresol and 9 mL of HF/g of peptide resin). During the cleavage the temperature of the ice bath was maintained between −5 and −10 °C for 30 min and then at −2 °C for 60−70 min.

The peptides were analyzed on the analytical HPLC system using three different eluting solvent pairs. Mixture 1: (A) 0.1% (v/v) TFA in water, (B) 0.08% or 0.1% (v/v) TFA in ACN. Mixture 2: (A) 0.1% (v/v) TFA in water, (B) 0.05% or 0.1% (v/v) TFA in IPA. Mixture 3: (A) 10 mM potassium phosphate buffer (pH 2.74), (B) ACN. In all cases, Vydac (The Separations Group; Hesperia, CA) reversed-phase columns were used (4.6 × 250 mm, C18, 300-Å pore size 5-μm particle size) with 1 mL/min flow rate, and the gradient formed with solvent B varied between 0.25% and 1%/min.

Folding/oxidation of the peptides was achieved in one of the following two "oxidation cocktails": (1) Ammonium acetate buffer (0.2 M, pH 8) containing 0.5 M guanidine hydrochloride and DTT (4−6-fold molar excess relative to the peptide) or (2) potassium phosphate buffer (0.05 M, pH 7.9−8.2) containing 0.5 M guanidine hydrochloride, DTT (4−6 mol/mol of peptide), and cysteine (10 mol/mol of peptide). Each oxidation procedure was started at room temperature in a concentrated solution, and after a 1-h reaction the mixture was diluted with water 6-fold to obtain the above described concentrations, and the solution was stirred at 4 °C for several days. The concentration of the reduced, crude peptide in the diluted solution was 2 mg/mL (corresponding to 0.3−0.7 mmol/L).

The progress of the oxidations was followed by HPLC (disappearance of the reduced starting material and the increase of the new product was checked at 1−2 day intervals) and by the Ellman reaction (upon completion of the reaction, no free sulfhydryl was present). Upon completion of the oxidation/folding, the reaction mixtures were acidified (pH 3−3.5), with either acetic acid or phosphoric acid, and lyophilized. The solid residues were redissolved in a small volume of water (<50 mL) and submitted to gel filtration on Sephadex G25 columns (2−5-cm diameter, 50−80-cm length) using 0.5 M acetic acid as eluent. The fractions containing the peptide monomer were lyophilized.

The final purification of each peptide was achieved using either a Rainin Dynamax preparative column (40.4 × 300 mm, C18, 300-Å pore size, 12−15-μm particle size) or a YMC (Wilmington, NC) preparative column (70 × 600 mm, C18, 200-Å pore size, 10−12-μm particle size). The flow rate varied between 40 and 90 mL/min, the gradients formed with solvent B were 0.25−1% B/mL. Smaller amounts of peptides (<5 mg) were purified on a Vydac column (22 ×

250 mm, C18, 300-Å pore size, 10-μm particle size) at a flow rate of 22 mL/min. The main principle in column selection was to avoid overloading as much as possible. We found that solvent mixture 3 (phosphate buffer/ACN) was better for the separation of the monomer from the polymers, and in some cases this system alone provided products with adequate purity (95+%). In such cases, the phosphate-containing peptides were desalted by gel filtration on a Sephadex G25 column with 0.5−1.0 M acetic acid as eluting solvent. When the phosphate/ACN system did not result in greater than 95% purity, a second preparative HPLC purification was performed using solvent mixture 1 (0.1% TFA/water/ACN).

Our standard HPLC-based analytical technique was modified in order to detect polymerlike impurities. The chromatograms of certain peptides showed 98+% purity when 1−5 μg was injected, but when 25 μg or more material was injected (at slightly overloading conditions), the polymers trailing the major peak were clearly distinguishable from the baseline. The reevaluated chromatograms indicated that the product purity was actually less than 90%. (In these cases a second HPLC purification was performed; see above.)

The amino acid composition of each of the purified peptides was determined by hydrolyzing a peptide with 6 N HCl *in vacuo* and analyzing the hydrolyzate on a Beckman Model 119C amino acid analyzer. The disulfide bond arrangements of the synthetic peptides were determined as described elsewhere (Chung et al., 1995).

Binding Assays. ^{125}I-SNX-111 was prepared by the Iodogen method (Fraker & Speck, 1978) and purified by reversed-phase HPLC and used in binding assays as described (Kristipati et al., 1994). Briefly, ^{125}I-SNX-111 (10 pM) was incubated at room temperature with 5 μg of rat brain synaptosomal membranes in a total volume of 0.5 mL of 20 mM HEPES buffer, pH 7.2, containing 75 mM NaCl, 0.1 mM EDTA, 0.1 mM EGTA, 2 μM leupeptin, 0.5 unit of aprotinin, and 0.1% BSA for 30 min. The reaction was terminated by adding 3 mL of chilled washing buffer (20 mM HEPES buffer, pH 7.2, 125 mM NaCl, and 0.1% BSA) and separating the membrane-bound radioactivity on glass fiber filters that were presoaked in 0.6% polyethylenimine. Filters were washed twice with ice-cold washing buffer (3 mL) and counted in a Model P-5000 γ counter (Beckman, Palo Alto, CA) at 75% counting efficiency. Complete displacement curves were generated for each analog and IC_{50} values for competition with ^{125}I-SNX-111 were determined using a four-parameter logistic equation.

RESULTS AND DISCUSSION

Synthesis of SNX-111 and Analogs. In view of the very low yields (≪1%) reported for the synthesis of the *Conus magus* peptide MVIIA (Olivera et al., 1987), we reinvestigated every step of the synthetic process with the aim of improving the overall yield significantly. The cycles of solid-phase synthesis were optimized on our ABI Model 430A peptide synthesizer according to the recommendations of Yamashiro and Li (1988). This modification resulted in an overall coupling yield better than 96% after 25 cycles. Cleavage of the peptides from the resin in liquid HF was done in one step in the presence of *p*-cresol as the scavenger. Careful monitoring of the temperature during cleavage was found to be a critical factor for good yields. The use of the "low/high HF" method (Tam et al., 1983) provided no noticeable advantage.

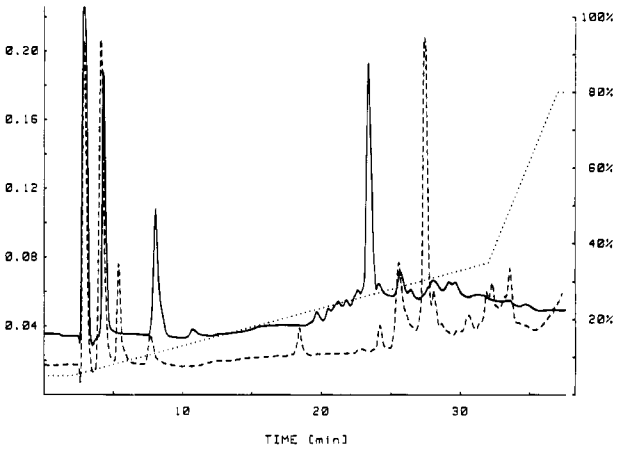

FIGURE 1: HPLC chromatogram illustrating the retention time changes during the oxidation of [Ala^{21}]-SNX-111. Dashed line, the oxidation mixture at the start; solid line, the oxidation mixture after 2 days. The peak at 27.4 min is the reduced peptide and the peak at 23.3 min is the folded, three-disulfide-bridged product. This particular oxidation was stopped after 3 days, when no further changes were observed. The dotted line shows the gradient formed with ACN. Left margin: 1.0 AUFS at 214 nm; right margin: solvent B.

Significant improvement in the yields of the peptides was also achieved by optimizing the conditions for folding and oxidation after cleavage from the resin. Air oxidation was found to be slow at 4 °C in a buffered solution (pH 8), requiring 2−6 days for completion. However, low temperature had a favorable effect on the final yield since many of the peptides tended to polymerize at room temperature. Whereas ammonium acetate served as a convenient buffer in view of its volatility, several of the peptides folded significantly better in potassium phosphate buffer in the presence of cysteine as the oxidation mediating agent. It is interesting that DTT alone did not suffice; the yield of the product was very poor when no cysteine was added. Anaerobic oxidation with the mixture of the oxidized and reduced forms of glutathione offered no improvement compared to the ammonium acetate−cysteine procedure. In spite of the potential for generating 15 different isomers during random air oxidation, all the peptides folded to yield only one major product and no other isomers were obtained in significant amounts. The disulfide bridging of the major products corresponded to the arrangement previously elucidated for the related conopeptide, GVIA (see below). Those analogs which folded poorly appeared to polymerize instead of forming the isomeric disulfide arrangements. Since all the peptides polymerized extensively, we studied the effect of peptide concentration on the yield of the desired product. A concentration of 2 mg/mL crude peptide, corresponding to approximately 0.5 mM, was found to be suitable. Typical changes of the chromatographic behavior of the compounds during the oxidation are illustrated in Figure 1.

The synthetic peptides were purified by reversed-phase HPLC. Final purification was achieved using potassium phosphate (pH 2.74)/ACN elution, which proved superior to the usual 0.1% aqueous TFA/ACN solvent system. The protocols described above worked reasonably well for a wide range of analogs of SNX-111 (MVIIA). The yield of the purified product varied between 3% and 15% of the calculated theoretical peptide load. The best results were obtained with SNX-111, which folded well in both oxidation buffer systems. Some analogs like SNX-195 (Ala^{24}-SNX-111) polymerized extensively in the ammonium acetate

Table 2: HPLC Characterization of the Synthetic SNX-111 Analogs

compound		capacity factor (k') solvent system I[a]	solvent system II[b]
SNX-111		4.61	5.66
SNX-190	[Ala^4]-SNX-111	4.75	6.16
SNX-191	[Ala^2]-SNX-111	4.88	6.32
SNX-194	[Nle^{12}]-SNX-111	6.31	6.72
SNX-195	[Ala^{24}]-SNX-111	4.72	6.58
SNX-198	[Ala^{21}]-SNX-111	4.84	7.11
SNX-199	[Ala^{10}]-SNX-111	5.44	7.13
SNX-200	[Ala^7]-SNX-111	4.85	6.29
SNX-201	[Arg^{9}Lys^{10}Thr^{11}Ser^{12}]-SNX-111	2.34	3.29
SNX-202	[Ser^{9}Arg^{10}Leu^{11}Met^{12}]-SNX-183	5.39	7.00
SNX-220	Ac-SNX-111	5.24	7.96
SNX-257	[Phe^{13}]-SNX-111	6.39	8.03
SNX-259	[ITyr^{13}]-SNX-111	5.96	7.64
SNX-273	[Ala^{12}]-SNX-111	3.79	3.41
SNX-279	[Met(O)^{12}]-SNX-111	3.57	4.68
SNX-288	[Ala^{11}]-SNX-111	2.74	4.12
SNX-308	[Ala^{14}]-SNX-111	4.91	6.26

[a] System I: 0 min, 100% solvent A; 30 min, 22.9% solvent A/77.1% solvent B. [b] System II: 0 min, 100% solvent C; 30 min, 80% solvent C/20% solvent D.

buffer and folded acceptably only in the phosphate buffer. The retention times in the two solvent systems for all the synthetic peptides used in this study are listed in Table 2. Amino acid analysis of acid hydrolyzates of the purified peptides agreed well with the theoretical values (Table 3).

Since, in principle, random air oxidation can generate 15 isomers, each with a unique arrangement of three disulfide bonds, complete characterization of these synthetic peptides requires the elucidation of the disulfide bridging pattern. The strategy that we developed involves digestion of the peptide with chymotrypsin, trypsin, and/or submaxillary protease, separation of the peptide fragments by reversed-phase HPLC, followed by amino acid analysis and sequencing (Chung et al., 1995). These studies showed that the disulfide bridges in SNX-111 are between C^1 and C^{16}, C^8 and C^{20}, and C^{15} and C^{25}, which is the same arrangement reported for the peptide GVIA from *Conus geographus* (Nishiuchi et al., 1986; Davis et al., 1993). The same arrangement of disulfide bonds was found to be present in all the analogs synthesized for use in the present investigation. To our kowledge, this is the first report demonstrating that the disulfide bridge arrangement of SNX-111 (MVIIA) is the same as that assumed hitherto on the basis of similarity to conopeptide GVIA.

Structure–Function Relationships. Although ω-conopeptide GVIA has been used extensively as a pharmacological tool for the identification of N-type VSCC, there is little information concerning the structural features important for the interaction of the peptide with the target N-type VSCC. Sabo et al. (1992) reported that none of the disulfide bridges of GVIA could be eliminated without severe loss of potency as measured in a goldfish lethality assay. The synthetic conopeptide SNX-111 also blocks N-type VSCC in a highly selective fashion but binds to N-type VSCC-rich synaptosomes reversibly, unlike GVIA, which binds essentially irreversibly (Olivera et al., 1987; Kristipati et al., 1994). Furthermore, SNX-111 was found to be highly efficacious in preventing the neuronal loss that occurs following global (Valentino et al., 1993) as well as focal (Xue et al., 1993; Buchan et al., 1994) ischemia. In view of the potential clinical significance of the actions of SNX-111, we have investigated the structural features of SNX-111 responsible for its highly selective interaction with N-type VSCC quantitated by the specific binding affinity to purified synaptosomes.

Role of the Basic Amino Acid Residues. SNX-111 is a highly basic peptide containing four lysines and two arginines with a calculated p*I* of 11.2. Since Ca^{2+} inhibits the binding of radiolabeled SNX-111 to N-type VSCC in rat brain synaptosomal preparations (Kristipati et al., 1994), the positively charged side chains of lysine and arginine are likely to be involved in the binding and blockage of N-type VSCC. The importance of each of these basic residues for the function of SNX-111 was evaluated by replacing each with an alanine residue. As the results in Figure 2 and Table 4 show, the lysine residue in position 2, the arginines at position 10 and 21, and the N-terminal amino group appear to be the most important basic moieties for optimal binding of SNX-111 to N-type VSCC. The lysines in positions 4 and 7 are of lesser importance, and the lysine in position 24 makes only a minor contribution. The latter is a surprising result in view of the conservation of a basic residue in this position in all the naturally occurring ω-conopeptides (Ramilo et al., 1992).

Table 3: Amino Acid Analysis of the Synthetic SNX-111 Analogs

compound	Ala	Arg	Asp	Cys[a]	Gly	Leu	Lys	Met	Ser[a]	Thr[a]	Tyr	Xxx
SNX-111	1.07 (1)	1.93 (2)	1.07 (1)	5.29 (6)	4.05 (4)	1.02 (1)	4.01 (4)	1.03 (1)	2.63 (3)	1.06 (1)	0.96 (1)	
SNX-190	2.07 (2)	1.88 (2)	1.01 (1)	5.06 (6)	3.99 (4)	1.04 (1)	2.97 (3)	1.00 (1)	2.70 (3)	0.97 (1)	0.94 (1)	
SNX-191	2.08 (2)	1.97 (2)	0.77 (1)	5.21 (6)	4.02 (4)	1.03 (1)	2.96 (3)	0.98 (1)	2.78 (3)	1.00 (1)	0.96 (1)	
SNX-194	1.09 (1)	1.94 (2)	0.98 (1)	4.59 (6)	4.14 (4)	0.98 (1)	4.07 (4)		2.52 (3)	1.02 (1)	1.03 (1)	1[b] (1)
SNX-195	2.02 (2)	1.99 (2)	1.02 (1)	4.98 (6)	3.89 (4)	1.01 (1)	3.06 (3)	0.98 (1)	2.45 (3)	1.02 (1)	0.95 (1)	
SNX-198	2.09 (2)	1.02 (1)	1.12 (1)	5.43 (6)	4.08 (4)	1.01 (1)	3.83 (4)	0.97 (1)	2.90 (3)	1.03 (1)	0.94 (1)	
SNX-199	2.08 (2)	0.98 (1)	1.11 (1)	5.23 (6)	4.01 (4)	1.03 (1)	3.96 (4)	1.01 (1)	2.95 (3)	1.05 (1)	0.95 (1)	
SNX-200	2.08 (2)	1.96 (2)	1.04 (1)	5.05 (6)	3.92 (4)	1.02 (1)	2.95 (3)	0.95 (1)	2.78 (3)	1.01 (1)	0.93 (1)	
SNX-201	1.06 (1)	2.03 (2)	1.03 (1)	5.13 (6)	3.96 (4)		4.97 (5)		2.56 (3)	2.01 (2)	1.06 (1)	
SNX-202		2.03 (2)	0.97 (1)	5.11 (6)	3.87 (4)	2.04 (2)	2.99 (3)	0.97 (1)	4.02 (5)		0.92 (1)	1.02[c] (1)
SNX-220	1.07 (1)	1.95 (2)	1.15 (1)	5.30 (6)	3.92 (4)	1.04 (1)	3.99 (4)	0.98 (1)	2.74 (3)	1.13 (1)	0.92 (1)	
SNX-257	0.99 (1)	1.93 (2)	0.72 (1)	5.47 (6)	4.17 (4)	0.97 (1)	4.08 (4)	0.91 (1)	2.65 (3)	0.88 (1)		0.93[d] (1)
SNX-259	1.09 (1)	1.98 (2)	1.10 (1)	5.48 (6)	4.07 (4)	1.02 (1)	3.86 (4)	0.97 (1)	2.89 (3)	1.02 (1)	0.95[f] (1)	
SNX-273	2.08 (2)	1.99 (2)	1.03 (1)	5.23 (6)	3.93 (4)	1.01 (1)	4.06 (4)		2.46 (3)	1.01 (1)	0.99 (1)	
SNX-279	1.10 (1)	1.91 (2)	1.02 (1)	4.64 (6)	4.18 (4)	0.99 (1)	4.05 (4)	0.97[e] (1)	2.48 (3)	1.04 (1)	0.84 (1)	
SNX-288	2.06 (2)	2.02 (2)	1.06 (1)	5.27 (6)	3.94 (4)		4.03 (4)	0.97 (1)	2.75 (3)	1.00 (1)	0.96 (1)	
SNX-308	2.05 (2)	1.98 (2)		5.16 (6)	3.91 (4)	1.02 (1)	4.05 (4)	1.00 (1)	2.51 (3)	0.97 (1)	0.94 (1)	

[a] Cys, Ser and Thr are partially destroyed during the hydrolysis. The Thr values are somewhat higher than expected due to the overlapping of the Thr peak with the much larger Ser peak. [b] Nle. [c] Glu. [d] Phe. [e] Met (0) is converted to Met during the hydrolysis. [f] Iodotyrosine is converted to tyrosine during the hydrolysis.

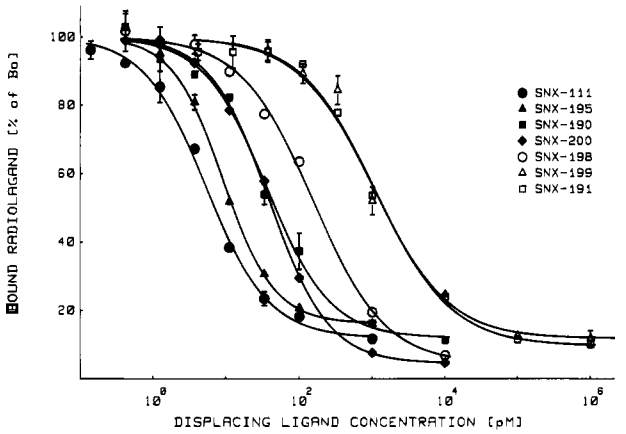

FIGURE 2: ^{125}I-SNX-111 binding displacement by SNX-111 and its analogs. Analogs containing an alanine residue in place of each of the basic residues present in SNX-111 were compared with SNX-111 in the competitive binding assay as described under Experimental Procedures. The error bars show the standard deviation of replicate samples at each competing ligand concentration. The four-parametric logistic function fitted to data indicated a "slope" value close to 1.0 for all compounds.

Table 4: Effect of Elimination of Positive Charges on the Binding Potency of SNX-111

peptide	substitution	IC_{50}[a] (pM)	relative potency[b] (%)
SNX-111		7.9	100
SNX-220 (N^{α}-acetyl-SNX-111)	$NH_2 \rightarrow$ AcNH	210	3.8
SNX-191 (A^2-SNX-111)	Lys → Ala	670	1.2
SNX-190 (A^4-SNX-111)	Lys → Ala	36	22
SNX-200 (A^7-SNX-111)	Lys → Ala	47	17
SNX-199 (A^{10}-SNX-111)	Arg → Ala	300	2.6
SNX-198 (A^{21}-SNX-111)	Arg → Ala	160	5.0
SNX-195 (A^{24}-SNX-111)	Lys → Ala	9.8	81

[a] IC_{50} values were determined from complete displacement curves like the ones shown in Figure 2. The numbers in the table are the geometric means of several assays. [b] Relative potency values were determined by averaging the ratios of the IC_{50} values of SNX-111 and the analogs from repeated experiments.

Table 5: Effect of Selective Cleavage of Peptide Bonds on the Binding Potencies of SNX-111 and SNX-183[a]

peptide	relative potency (%)
SNX-111	100
SNX-111 cleaved at Y^{13} D^{14}	1.4
des-M^{12} Y^{13}-SNX-111	0.002
SNX-183	100
SNX-183 cleaved at Y^{13} D^{14}	3
SNX-183 cleaved at L^3 K^4, G^5 Q^6, and Y^{13} D^{14}	1

[a] The nicked derivatives were generated by treating SNX-111 or SNX-183 with chymotrypsin (peptide:enzyme = 25:1) in 10 mM phosphate buffer, pH 7 at 37 °C, and isolated by reversed-phase HPLC. Structures were confirmed by amino acid analysis and sequencing (data not shown). Relative potencies (i.e., relative to the intact peptide) were calculated from IC_{50} values obtained from displacement curves as described in Table 4.

Role of the Middle Segment. The selective cleavage of the peptide link between tyrosine^{13} and aspartic acid^{14} by mild treatment with chymotrypsin results in a 99% decrease in binding affinity. The removal of the dipeptide Met^{12}-Tyr^{13} by more extended treatment leads to almost total loss of affinity (Table 5). Thus the rigidity conferred by the unique three-disulfide-bond arrangement in SNX-111 appears to be highly important for the function of SNX-111 as an N-type VSCC antagonist. These results were reinforced by similar findings with SNX-183, the synthetic peptide corresponding to ω-conopeptide S-VI-B isolated from the venom of *Conus striatus* (Ramilo et al., 1992). Cleavage of the Tyr^{13}-Asp^{14} bond in SNX-183 decreased the binding potency by 97% but additional cleavages between Leu^3-Lys^4 and Gly^5-Gln^6 decreased the affinity only a little further (Table 5). These results led to a more thorough examination of the residues Ser^9-Arg^{10}-Leu^{11}-Met^{12}-Tyr^{13}-Asp^{14} in the sequence of SNX-111, which represents the major difference between SNX-111 and SNX-183. Single amino acid replacement of each of the five residues from Arg^{10} to Asp^{14} in SNX-111 revealed that Tyr^{13} and Leu^{11} are the most important in this segment (Table 6). Omission of the phenolic hydroxyl group of Tyr^{13} by replacement with Phe^{13} (SNX-257) reduced the binding affinity to 0.5% that of SNX-111, but substitution of Tyr^{13} with monoiodotyrosine (SNX-259) caused only a 40% reduction of the binding affinity. This result suggests that the phenolic hydroxyl group of the tyrosine residue is the critical function in the interaction of this side chain with the calcium channel. Substitution of Met^{12} with the isosteric norleucine residue (SNX-194) or with alanine (SNX-273) had no adverse effect on the binding. Even the replacement of the hydrophobic side chain of methionine in position 12 by the polar Met $(0)^{12}$ caused only a 5-fold decrease in affinity, whereas substitution of Leu^{11} by Ala^{11} resulted in a dramatic 100-fold loss of affinity.

Table 6: Relative Potencies of Analogs of SNX-111 Substituted in Positions 10−14

peptide	substitution	relative potency[a] (%)
SNX-111		100
SNX-199 (A^{10}-SNX-111)	Arg → Ala	2.6
SNX-288 (A^{11}-SNX-111)	Leu → Ala	0.97
SNX-194 (Nle^{12}-SNX-111)	Met → Nle	60
SNX-273 (Ala^{12}-SNX-111)	Met → Ala	80
SNX-279 ($Met(0)^{12}$-SNX-111)	Met → Met(O)	16
SNX-257 (Phe^{13}-SNX-111)	Tyr → Phe	0.53
SNX-259 ($ITyr^{13}$-SNX-111)	Tyr → ITyr	57
SNX-308 (A^{14}-SNX-111)	Asp → Ala	24

[a] Relative potencies were determined from IC_{50} values as described in Table 4.

The importance of the central segment, Ser^9-Arg^{10}-Leu^{11}-Met^{12}, for binding affinity of SNX-111 to N-type VSCC in rat brain synaptosomes is also apparent from a comparison of the structure of SNX-111 with SNX-183, which binds with considerably lower affinity (IC_{50} = 1700 pM). Since five out of the first eight residues and 12 out of the 14 carboxy-terminal residues are identical between SNX-111 and SNX-183, the major difference, which may be responsible for the differences in affinity, is in the middle four residues, namely, residues 9−12. To further evaluate the importance of this segment, we constructed two hybrid molecules by swapping the middle domains of SNX-111 and SNX-183 (Table 7). Substitution of the residues Arg^9-Lys^{10}-Thr^{11}-Ser^{12} in SNX-183 with Ser^9-Arg^{10}-Leu^{11}-Met^{12} from SNX-111 created the hybrid SNX-202, which displayed a 38-fold higher affinity for N-type VSCC compared to SNX-183. A modest but significant reduction in the affinity of SNX-111 resulted when the residues Ser^9-Arg^{10}-Leu^{11}-Met^{12} were replaced by Arg^8-Lys^{10}-Thr^{11}-Ser^{12} to generate the hybrid SNX-201.

Three-Dimensional Conformation and Binding Interactions. All the conopeptide analogs of the N-type VSCC blocker SNX-111 described here have the same disulfide

Table 7: Relative Potencies of SNX-111/SNX-183 Hybrids

peptide		relative potency[a] (%)
SNX-111		100
SNX-183		0.6
SNX-201	($R^9K^{10}T^{11}S^{12}$-SNX-111)	24
SNX-202	($S^9R^{10}L^{11}M^{12}$-SNX-183)	23

[a] Relative potencies were derived from IC_{50} values obtained from displacement curves similar to those in Figure 2 as described in Table 4.

bridge arrangement (Chung et al., 1995). The three disulfide bridges restrain the peptide chain in a unique and relatively rigid three-dimensional structure. We have recently determined the solution structure of the ω-conopeptide GVIA (Davis et al., 1993) and MVIIC (Farr-Jones et al., 1995) using two-dimensional NMR in combination with distance geometry and restrained molecular dynamics. The very similar backbone structures, and also the identity of the disulfide bridge pattern of these two peptides, suggest a similar three-dimensional structure for SNX-111 which is highly homologous to that of MVIIC (Olivera et al., 1994). It is highly likely that the backbone structures of the analogs are similar to the structure of SNX-111 since all of them have the same disulfide bridge pattern. Therefore, the significant differences observed in binding potencies of certain analogs probably arise from the structure features of the amino acid side chains that were replaced in the analogs. It appears that the very high binding affinity of SNX-111 to purified synaptosomes, and consequently to N-type VSCC, is derived in large part from the phenolic group of Tyr^{13}, the hydrophobic side chain of Leu^{11}, and the positively charged side chains of Lys^2, Arg^{10}, and Arg^{21}, in addition to the amino-terminal α-amino group. Comparison of the binding potencies of SNX-111 with that of SNX-183 and the hybrid molecule SNX-202 reinforce the importance of the middle segment, Ser^9-Arg^{10}-Leu^{11}-Met^{12}, for the selective interaction with N-type VSCC. These results suggest that the rigid framework of the three disulfide bridges enables the specific interaction of SNX-111 with N-type VSCC through the middle segment, Ser^9-Arg^{10}-Leu^{11}-Met^{12}-Tyr^{13}-Asp^{14}, and this interaction may position the basic groups at Lys^2 and Arg^{21} and the α-amino group at the Ca^{2+} binding site of the channel, thereby blocking Ca^{2+} influx through the channel pore. It should be noted that the high binding potency retained by the hybrid peptide SNX-201 suggests either a cooperative involvement of all the other amino acid residues in SNX-111 or maybe an alternative way the peptide can interact with the channel. Elucidation of the structural features involved in the interaction between the conopeptide, SNX-111, and the calcium channel, as well as the three-dimensional structure of the conopeptide, should greatly facilitate the design of peptidomimetics for clinical applications.

NOTE ADDED IN PROOF

In confirmation of our results regarding the importance of the tyrosine residue in position 13 and of the lysine in position 2, recently, after the submission of our manuscript, two articles have been published (Kim et al., 1994, 1995) addressing the structure–activity relationship for ω-conopeptides. The investigators, applying single amino acid replacement in ω-conopeptides GVIA and MVIIA, found significant binding activity loss in chick brain synaptic plasma membranes.

ACKNOWLEDGMENT

We thank Diego Silva and Louis Brogley for their skillful technical assistance and John Bell and George Miljanich for many useful discussions.

REFERENCES

Buchan, A. M., Gertler, S. Z., Li, H., Xue, D., Huang, Z.-G., Sun, P., Chaundy, K. E., Barnes, K., Adams, B., Todd, M., & Lesiuk, H. J. (1994) *J. Cereb. Blood Flow Metab. 14*, 903–910.

Chung, D., Gaur, S., Bell, J. R., Ramachandran, J., & Nadasdi, L. (1995) *Int. J. Pept. Protein Res.*, memorial issue for Dr. J. A. Meienhofer (in press).

Davis, J. H., Bradley, E. K., Miljanich, G. P., Nadasdi, L., Ramachandran, J., & Basus, V. J. (1993) *Biochemistry 32*, 7396–7405.

Farr-Jones, S., Miljanich, G. P., Nadasdi, L., Ramachandran, J., & Basus, V. J. (1995) *J. Mol. Biol. 248*, 106–124.

Fraker, P. J., & Speck, J. C., Jr. (1978) *Biochem. Biophys. Res. Commun. 80*, 849–857.

Gohil, K., Bowersox, S., Singh, T., Ramachandran, J., & Miljanich, G. (1993) *Soc. Neurosci. Abstr. 19*, 235.

Gray, W. R., Olivera, B. M., & Cruz, L. J. (1988) *Annu. Rev. Biochem. 57*, 665–700.

Hillyard, D. R., Monje, V. D., Mintz, I. M., Bean, B. P., Nadasdi, L., Ramachandran, J., Miljanich, G. P., Azimi-Zoonooz, A., McIntosh, J. M., Cruz, L. J., Imperial, J. S., & Olivera, B. M. (1992) *Neuron 9*, 69–77.

Kim, J. I., Takahashi, M., Ogura, A., Kohno, T., Kudo, Y., & Sato, K. (1994) *J. Biol. Chem. 269*, 23876–23878.

Kim, J. I., Takahashi, M., Ohtake, A., Wakamiya, A., & Sato, K. (1995) *Biochem. Biophys. Res. Commun. 206*, 449–454.

Kristipati, R., Nadasdi, L., Tarczy-Hornoch, K., Lau, K., Miljanich, G. P., Ramachandran, J., & Bell, J. R. (1994) *Mol. Cell. Neurosci. 5*, 219–228.

Miller, R. J. (1992) *J. Biol. Chem. 267*, 1403–1406.

Nishiuchi, Y., Lumagaye, K., Noda, Y., Watanabe, T. X., & Sakakibara, S. (1986) *Biopolymers 25*, S61–S68.

Olivera, B. M., Cruz, L. J., de Santos, V., LeCheminant, G., Griffin, D., Zeikus, R., McIntosh, J. M., Galyean, R., Varga, J., Gray, W. R., & Rivier, J. (1987) *Biochemistry 26*, 2086–2090.

Olivera, B. M., Rivier, J., Clark, C., Ramilo, C. A., Corpuz, G. P., Abogadie, F. C., Mena, E. E. Woodward, S. R., Hillyard, D. R., & Cruz, L. J. (1990) *Science 249*, 257–263.

Olivera, B. M., Ramachandran, J., Miljanich, G. P., & Adams, M. E. (1994) *Annu. Rev. Biochem. 63*, 823–867.

Ramachandran, J., Nadasdi, L., Gohil, K., Kristipati, R., Tarczy-Hornoch, K., Gaur, S., Singh, T., Bell, J. R., & Miljanich, G. P. (1993) in *Perspectives in Medicinal Chemistry* (Testa, B., Kyburz, E., Fuhrer, W., & Geiger, R., Eds.) pp 375–388, VCH, New York.

Ramilo, C. A., Zafarella, G. C., Nadasdi, L., Hammerland, L. G., Yoshikami, D., Gray, W. R., Kristipati, R., Ramachandran, J., Miljanich, G. P., Olivera, B. M., & Cruz, L. J. (1992) *Biochemistry 31*, 9919–9926.

Sabo, T., Gilon, C., Shafferman, A., & Elhanaty, E. (1992) in *Peptides*, Proceedings of the Twelfth American Peptide Symposium 1991, Cambridge, MA (Smith, J. A., & Rivier, J. E., Eds.) pp 159–160, ESCOM, Leiden, The Netherlands.

Smith, M. L., & Siesjo, B. K. (1992) in *Pharmacology of Cerebral Ischemia*, eds. (Krieglstein, J., & Oberpilcher, H., Eds.) pp 161–167, Wissenschaftliche Verlagsgesellschaft Stuttgart, Germany.

Snutch, T. P., & Reiner, P. B. (1992) *Curr. Opin. Neurobiol. 2*, 247–253.

Tam, J. P., Heath, W. F., & Merrifield, R. B. (1983) *J. Am. Chem. Soc. 105*, 6442–6445.

Tsien, R. W., Elinor, P. T., & Horne, W. A. (1991) *Trends Pharmacol. Sci. 12*, 349.

Valentino, K., Newcomb, R., Gadbois, T., Singh, T., Bowersox, S., Bitner, S., Justice, A., Yamashiro, D., Hoffman, B. B., Ciaranello, R., Miljanich, G., & Ramachandran, J. (1993) *Proc. Natl. Acad. Sci. U.S.A. 90*, 7894–7897.

Xue, D., Huang, Z. G., Barnes, K., Lesiuk, H., Smith, K. E., & Buchan, A. M. (1993) in *Soc. Neurosci. Abstr. 19*, 1643.

Yamashiro, D., & Li, C. H. (1988) *Int. J. Pept. Protein Res. 31*, 322–334.

BI950781U